

Impact of slepton generation mixing on the search for sneutrinos

Lepton flavour violation in sneutrino production and decays in the general MSSM

K. Hidaka

Department of Physics, Tokyo Gakugei University, Koganei, Tokyo 184–8501, Japan

Abstract. We perform a systematic study of sneutrino production and decays in the Minimal Supersymmetric Standard Model (MSSM) with slepton generation mixing. We study bosonic decays like $\tilde{\nu} \rightarrow \tilde{\ell}^- + W^+/H^+$ as well as fermionic ones. We show that the effect of slepton generation mixing on the sneutrino production and decays can be quite large in a significant part of the MSSM parameter space despite the very strong experimental limits on lepton flavour violating processes. This could have an important impact on the search for sneutrinos and the determination of the MSSM parameters at future colliders, such as LHC, ILC, CLIC and muon collider.

PACS. 12.15.Ji Applications of electroweak models to specific processes

1 Introduction

Systematic studies of decays of sneutrinos, the supersymmetric (SUSY) partners of neutrinos, in the Minimal Supersymmetric Standard Model (MSSM) have been performed already [1]. In these studies it is assumed that there is no generation mixing in the slepton sector. In this article based on [2] we study the effect of slepton generation mixing on the production and decays of the sneutrinos in the MSSM. Lepton flavour violating (LFV) productions and decays of SUSY particles have been studied for the case of slepton generation mixing [3]. Some of the studies are rather model dependent. Furthermore, so far no systematic study of LFV in sneutrino decays including bosonic decays has been performed. The aim of this article is to perform a systematic study of sneutrino production and decays including the bosonic decay modes in the general MSSM with LFV in slepton sector.

2 The model

First we summarize the MSSM parameters in our analysis. The most general charged slepton mass matrix including left-right mixing as well as flavour mixing in the basis of $\tilde{\ell}_{0\alpha} = (\tilde{e}_L, \tilde{\mu}_L, \tilde{\tau}_L, \tilde{e}_R, \tilde{\mu}_R, \tilde{\tau}_R)$, $\alpha = 1, \dots, 6$, is given by [2]:

$$M_{\tilde{\ell}}^2 = \begin{pmatrix} M_{LL}^2 & M_{RL}^{2\dagger} \\ M_{RL}^2 & M_{RR}^2 \end{pmatrix},$$

with

$$M_{LL,\alpha\beta}^2 = M_{L,\alpha\beta}^2 + m_Z^2 \cos(2\beta) \left(-\frac{1}{2} + \sin^2 \theta_W\right) \delta_{\alpha\beta}$$

$$+ m_{\tilde{\ell}_\alpha}^2 \delta_{\alpha\beta},$$

$$M_{RR,\alpha\beta}^2 = M_{E,\alpha\beta}^2 - m_Z^2 \cos(2\beta) \sin^2 \theta_W \delta_{\alpha\beta} + m_{\tilde{\ell}_\alpha}^2 \delta_{\alpha\beta},$$

$$M_{RL,\alpha\beta}^2 = v_1 A_{\beta\alpha} - m_{\ell_\alpha} \mu^* \tan \beta \delta_{\alpha\beta}.$$

The indices $\alpha, \beta = 1, 2, 3$ characterize the flavours e, μ, τ , respectively. M_L^2 and M_E^2 are the hermitean soft SUSY breaking mass matrices for left and right sleptons, respectively. $A_{\alpha\beta}$ are the trilinear soft SUSY breaking couplings of the sleptons and the Higgs boson: $\mathcal{L}_{\text{int}} = -A_{\alpha\beta} \tilde{\ell}_{\beta R}^\dagger \tilde{\ell}_{\alpha L} H_1^0 + A_{\alpha\beta} \tilde{\ell}_{\beta R}^\dagger \tilde{\nu}_{\alpha L} H_1^- + \dots$. μ is the higgsino mass parameter. v_1 and v_2 are the vacuum expectation values of the Higgs fields with $v_1 = \langle H_1^0 \rangle$, $v_2 = \langle H_2^0 \rangle$, and $\tan \beta \equiv v_2/v_1$. We work in a basis where the Yukawa coupling matrix $Y_{E,\alpha\beta}$ of the charged leptons is real and flavour diagonal with $Y_{E,\alpha\alpha} = m_{\ell_\alpha}/v_1 = \frac{g}{\sqrt{2}} \frac{m_{\ell_\alpha}}{m_W \cos \beta}$ ($\ell_\alpha = e, \mu, \tau$), with m_{ℓ_α} being the physical lepton masses and g the SU(2) gauge coupling. The physical mass eigenstates $\tilde{\ell}_i$, $i = 1, \dots, 6$, are given by $\tilde{\ell}_i = R_{i\alpha}^\ell \tilde{\ell}_{0\alpha}$. The mixing matrix R^ℓ and the physical mass eigenvalues are obtained by an unitary transformation $R^\ell M_{\tilde{\ell}}^2 R^{\ell\dagger} = \text{diag}(m_{\tilde{\ell}_1}^2, \dots, m_{\tilde{\ell}_6}^2)$, where $m_{\tilde{\ell}_i} < m_{\tilde{\ell}_j}$ for $i < j$. Similarly, the mass matrix for the sneutrinos, in the basis $\tilde{\nu}_{0\alpha} = (\tilde{\nu}_{eL}, \tilde{\nu}_{\mu L}, \tilde{\nu}_{\tau L}) \equiv (\tilde{\nu}_e, \tilde{\nu}_\mu, \tilde{\nu}_\tau)$, reads

$$M_{\tilde{\nu},\alpha\beta}^2 = M_{L,\alpha\beta}^2 + \frac{1}{2} m_Z^2 \cos(2\beta) \delta_{\alpha\beta} \quad (\alpha, \beta = 1, 2, 3),$$

where the physical mass eigenstates are given by $\tilde{\nu}_i = R_{i\alpha}^{\tilde{\nu}} \tilde{\nu}_{0\alpha}$, $i = 1, 2, 3$, ($m_{\tilde{\nu}_1} < m_{\tilde{\nu}_2} < m_{\tilde{\nu}_3}$).

The properties of the charginos $\tilde{\chi}_i^\pm$ ($i = 1, 2$, $m_{\tilde{\chi}_1^\pm} < m_{\tilde{\chi}_2^\pm}$) and neutralinos $\tilde{\chi}_k^0$ ($k = 1, \dots, 4$, $m_{\tilde{\chi}_1^0} < \dots < m_{\tilde{\chi}_4^0}$) are determined by the parameters M_2, M_1, μ

and $\tan\beta$, where M_2 and M_1 are the SU(2) and U(1) gaugino masses, respectively. Assuming gaugino mass unification we take $M_1 = (5/3)\tan^2\theta_W M_2$.

The possible fermionic and bosonic two-body decay modes of sneutrinos are

$$\begin{aligned}\tilde{\nu}_i &\longrightarrow \nu\tilde{\chi}_j^0, \ell_\alpha^-\tilde{\chi}_k^+, \\ \tilde{\nu}_i &\longrightarrow \tilde{\ell}_j^-W^+, \tilde{\ell}_j^-H^+.\end{aligned}$$

3 Constraints

In our analysis, we impose the following conditions on the MSSM parameter space in order to respect experimental and theoretical constraints which are described in detail in [2]:

- (i) The vacuum stability conditions [4], such as $|A_{\alpha\beta}|^2 < Y_{E,\gamma\gamma}^2(M_{L,\alpha\alpha}^2 + M_{E,\beta\beta}^2 + m_1^2)$, ($\alpha \neq \beta$; $\gamma = \text{Max}(\alpha, \beta)$; $\alpha, \beta = 1, 2, 3 = e, \mu, \tau$).
- (ii) Experimental limits on the LFV lepton decays: $B(\mu^- \rightarrow e^- \gamma) < 1.2 \times 10^{-11}$ (90% CL) [5], $B(\tau^- \rightarrow \mu^- \gamma) < 4.5 \times 10^{-8}$ (90% CL) [6], $B(\tau^- \rightarrow e^- \gamma) < 1.1 \times 10^{-7}$ (90% CL) [7], $B(\mu^- \rightarrow e^- e^+ e^-) < 1.0 \times 10^{-12}$ (90% CL) [8], $B(\tau^- \rightarrow \mu^- \mu^+ \mu^-) < 3.2 \times 10^{-8}$ (90% CL) [9], $B(\tau^- \rightarrow e^- e^+ e^-) < 3.6 \times 10^{-8}$ (90% CL) [9].
- (iii) Experimental limits on SUSY contributions to anomalous magnetic moments of leptons [10, 11]¹, e.g. $|\Delta a_\mu^{\text{SUSY}} - 287 \times 10^{-11}| < 178 \times 10^{-11}$ (95% CL).
- (iv) The LEP limits on SUSY particle masses.
- (v) The limit on m_{H^+} and $\tan\beta$ from the experimental data on $B(B_u^- \rightarrow \tau^- \bar{\nu}_\tau)$ [12].

It has been shown that in general the limit on the $\mu^- - e^-$ conversion rate is respected if the limit on $\mu \rightarrow e \gamma$ is fulfilled [13].

Condition (i) strongly constrains the trilinear couplings $A_{\alpha\beta}$, especially for small $\tan\beta$ where the lepton Yukawa couplings $Y_{E,\alpha\alpha}$ are small. (ii) strongly constrains the lepton flavour mixing parameters; e.g. in case of $\tilde{\mu} - \tilde{\tau}$ mixing the limit on $B(\tau^- \rightarrow \mu^- \gamma)$ strongly constrains the $\tilde{\mu} - \tilde{\tau}$ mixing parameters $M_{L,23}^2, M_{E,23}^2, A_{23}$ and A_{32} . The limit on $\Delta a_\mu^{\text{SUSY}}$ in (iii) is also important, e.g. it disfavours negative μ especially for large $\tan\beta$.

4 Numerical results

We take $\tan\beta, m_{H^+}, M_2, \mu, M_{L,\alpha\beta}^2, M_{E,\alpha\beta}^2$, and $A_{\alpha\beta}$ as the basic MSSM parameters at the weak scale. We assume them to be real. The LFV parameters are $M_{L,\alpha\beta}^2, M_{E,\alpha\beta}^2$, and $A_{\alpha\beta}$ with $\alpha \neq \beta$. We take the following $\tilde{\mu} - \tilde{\tau}$ mixing scenario as a reference scenario with LFV within reach of LHC and ILC:

¹ For the limit on SUSY contributions to anomalous magnetic moment of muon $\Delta a_\mu^{\text{SUSY}}$, we allow for an error at 95% CL for the difference between the experimental measurement and the SM prediction [11].

$\tan\beta = 20, m_{H^+} = 150\text{GeV}, M_2 = 650\text{GeV}, \mu = 150\text{GeV}, M_{L,11}^2 = (430\text{GeV})^2, M_{L,22}^2 = (410\text{GeV})^2, M_{L,33}^2 = (400\text{GeV})^2, M_{L,12}^2 = M_{L,13}^2 = (1\text{GeV})^2, M_{L,23}^2 = (61.2\text{GeV})^2, M_{E,11}^2 = (230\text{GeV})^2, M_{E,22}^2 = (210\text{GeV})^2, M_{E,33}^2 = (200\text{GeV})^2, M_{E,12}^2 = M_{E,13}^2 = (1\text{GeV})^2, M_{E,23}^2 = (22.4\text{GeV})^2, A_{23} = 25\text{GeV}, A_{33} = 150\text{GeV}$, and all the other $A_{\alpha\beta} = 0$.

In this scenario satisfying all the conditions (i)-(v) above we have:

$$m_{\tilde{\nu}_1} = 393\text{GeV}, m_{\tilde{\nu}_2} = 407\text{GeV}, m_{\tilde{\nu}_3} = 425\text{GeV},$$

$$\tilde{\nu}_1 = -0.36\tilde{\nu}_\mu + 0.93\tilde{\nu}_\tau \sim \tilde{\nu}_\tau,$$

$$\tilde{\nu}_2 = 0.93\tilde{\nu}_\mu + 0.36\tilde{\nu}_\tau \sim \tilde{\nu}_\mu,$$

$$\tilde{\nu}_3 \simeq \tilde{\nu}_e,$$

$$m_{\tilde{\ell}_1} = 204\text{GeV}, m_{\tilde{\ell}_2} = 215\text{GeV}, m_{\tilde{\ell}_3} = 234\text{GeV},$$

$$\tilde{\ell}_1 = -0.0029\tilde{\mu}_L + 0.033\tilde{\tau}_L - 0.12\tilde{\mu}_R + 0.99\tilde{\tau}_R \sim \tilde{\tau}_R,$$

$$\tilde{\ell}_2 = 0.0022\tilde{\mu}_L + 0.0040\tilde{\tau}_L + 0.99\tilde{\mu}_R + 0.12\tilde{\tau}_R \sim \tilde{\mu}_R,$$

$$\tilde{\ell}_3 \simeq \tilde{e}_R,$$

$$B(\tilde{\nu}_1 \rightarrow \mu^- + \tilde{\chi}_1^+) = 0.014, B(\tilde{\nu}_1 \rightarrow \tau^- + \tilde{\chi}_1^+) = 0.36,$$

$$B(\tilde{\nu}_1 \rightarrow \tilde{\ell}_1^- + H^+) = 0.48,$$

$$B(\tilde{\nu}_2 \rightarrow \mu^- + \tilde{\chi}_1^+) = 0.20, B(\tilde{\nu}_2 \rightarrow \tau^- + \tilde{\chi}_1^+) = 0.12,$$

$$B(\tilde{\nu}_2 \rightarrow \tilde{\ell}_1^- + H^+) = 0.38.$$

As $\tilde{\nu}_2 \sim \tilde{\nu}_\mu$ and $\tilde{\ell}_1^- \sim \tilde{\tau}_R^-$, the decays $\tilde{\nu}_2 \rightarrow \tau^- \tilde{\chi}_1^+$ and $\tilde{\nu}_2 \rightarrow \tilde{\ell}_1^- H^+$ are essentially LFV decays. Note that the branching ratios of these LFV decays are sizable in this scenario. The reason is as follows: The lighter neutralinos $\tilde{\chi}_{1,2}^0$ and the lighter chargino $\tilde{\chi}_1^\pm$ are dominantly higgsinos as $M_{1,2} \gg |\mu|$ in this scenario. Hence the fermionic decays into $\tilde{\chi}_{1,2}^0$ and $\tilde{\chi}_1^+$ are suppressed by the small lepton Yukawa couplings except for the decay into $\tau^- \tilde{\chi}_1^+$ which does not receive such a suppression because of the sizable τ Yukawa coupling $Y_{E,33}$ for large $\tan\beta$. This leads to an enhancement of the bosonic decays into the Higgs boson H^+ . Moreover the decay $\tilde{\nu}_2 (\sim \tilde{\nu}_\mu) \rightarrow \tilde{\ell}_1^- (\sim \tilde{\tau}_R^-) + H^+$ is enhanced by the sizable trilinear $\tilde{\nu}_\mu - \tilde{\tau}_R^+ - H_1^-$ coupling A_{23} (with $H_1^- = H^- \sin\beta$). Because of the sizable $\tilde{\nu}_\mu - \tilde{\nu}_\tau$ mixing term $M_{L,23}^2$ the $\tilde{\nu}_2$ has a significant $\tilde{\nu}_\tau$ component, which results in a further enhancement of this decay due to the large trilinear $\tilde{\nu}_\tau - \tilde{\tau}_R^+ - H_1^-$ coupling A_{33} ($= 150\text{GeV}$).

The decays of $\tilde{\nu}_1$ and $\tilde{\nu}_2$ into $\tilde{\ell}_{1,2}^- W^+$ are suppressed since $\tilde{\ell}_1^- \sim \tilde{\tau}_R^-$ and $\tilde{\ell}_2^- \sim \tilde{\mu}_R^-$.

4.1 $\tilde{\nu}$ decay branching ratios

We study the basic MSSM parameter dependences of the LFV sneutrino decay branching ratios for the reference scenario specified above. In Fig.1 we show contours of the LFV $\tilde{\nu}_2$ decay branching ratios in the $\mu - M_2$ plane. All basic parameters other than μ and M_2 are fixed as in the reference scenario specified above. We see that the LFV decay branching ratios $B(\tilde{\nu}_2 \rightarrow \tau^- \tilde{\chi}_1^+)$ and $B(\tilde{\nu}_2 \rightarrow \tilde{\ell}_1^- H^+)$ can be sizable in a significant part of the $\mu - M_2$ plane. The main reason for the increase of $B(\tilde{\nu}_2 \rightarrow \tilde{\ell}_1^- H^+)$ in the region $M_2 \gg \mu$ is that the partial widths for the decays into $\mu^- \tilde{\chi}_1^+$ and $\nu \tilde{\chi}_{1,2}^0$ decrease for increasing $|M_2/\mu|$ as the lighter

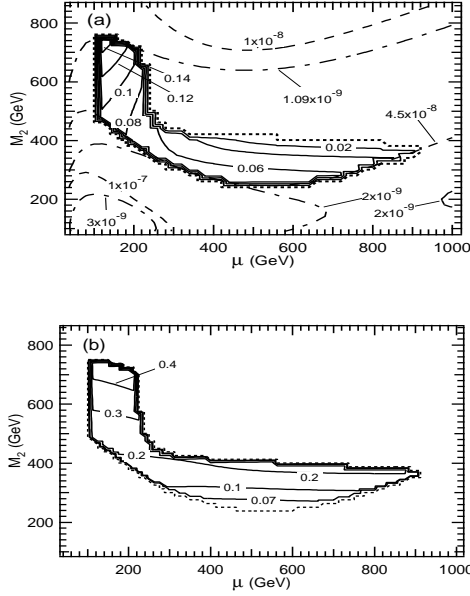


Fig. 1. Contours of (a) $B(\tilde{\nu}_2 \rightarrow \tau^- \tilde{\chi}_1^+)$ and (b) $B(\tilde{\nu}_2 \rightarrow \tilde{\ell}_1^- H^+)$ in the $\mu - M_2$ plane for our $\tilde{\mu} - \tilde{\tau}$ mixing scenario. The region with no solid contour-lines is excluded by the conditions (i) to (v) given in the text; negative μ region is excluded by the limit on Δa_μ^{SUSY} in (iii). The dashed and dash-dotted lines in (a) show contours of $B(\tau^- \rightarrow \mu^- \gamma)$ and Δa_μ^{SUSY} , respectively. Note that (iii) requires $1.09 \times 10^{-9} < \Delta a_\mu^{SUSY} < 4.65 \times 10^{-9}$.

chargino/neutralino states become more and more higgsino like. The $\tau^- \tilde{\chi}_1^+$ decay mode has a different behaviour due to the sizable τ Yukawa coupling for large $\tan \beta$. We remark that the limit on Δa_μ^{SUSY} excludes the region with $B(\tilde{\nu}_2 \rightarrow \tilde{\ell}_1^- H^+) \gtrsim 0.5$.

In the following we use the quantities $R_{L23} \equiv M_{L,23}^2 / ((M_{L,11}^2 + M_{L,22}^2 + M_{L,33}^2)/3)$ and $R_{A23} \equiv A_{23} / (|A_{11}| + |A_{22}| + |A_{33}|)/3)$ as a measure of LFV. In Fig.2 we present the R_{L23} dependence of $\tilde{\nu}_2$ decay branching ratios, where all basic parameters other than $M_{L,23}^2$ are fixed as in the reference scenario specified above. We see that the LFV decay branching ratios $B(\tilde{\nu}_2 \rightarrow \tau^- \tilde{\chi}_1^+)$ and $B(\tilde{\nu}_2 \rightarrow \tilde{\ell}_1^- H^+)$ can be large and very sensitive to R_{L23} . Note that $\tilde{\ell}_1^- \sim \tilde{\tau}_R^-$ and that the $\tilde{\nu}_\tau$ component in $\tilde{\nu}_2 (\sim \tilde{\nu}_\mu)$ increases with the increase of the $\tilde{\nu}_\mu - \tilde{\nu}_\tau$ mixing parameter $M_{L,23}^2$, which explains the behaviour of the branching ratios. Similarly we have found that $B(\tilde{\nu}_2 \rightarrow \tilde{\ell}_1^- H^+)$ can be very sensitive to R_{A23} ; this decay can be enhanced also by a sizable A_{23} as explained above. To exemplify this behaviour further, in Fig.3 we show the contours of these decay branching ratios in the $R_{L23} - R_{A23}$ plane, where all basic parameters other than $M_{L,23}^2$ and A_{23} are fixed as in the reference scenario specified above. As can be seen, these LFV decay branching ratios can be large in a sizable region of the $R_{L23} - R_{A23}$ plane and their dependences on R_{L23} and R_{A23} are quite remarkable and very different from each other. Hence, a simultaneous measurement of these two branching ratios could

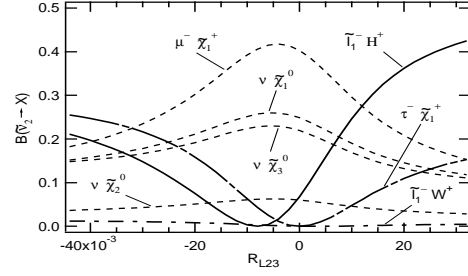


Fig. 2. R_{L23} dependence of $\tilde{\nu}_2$ decay branching ratios for our $\tilde{\mu} - \tilde{\tau}$ mixing scenario. The shown range of R_{L23} is the whole range allowed by the conditions (i) to (v) given in the text.

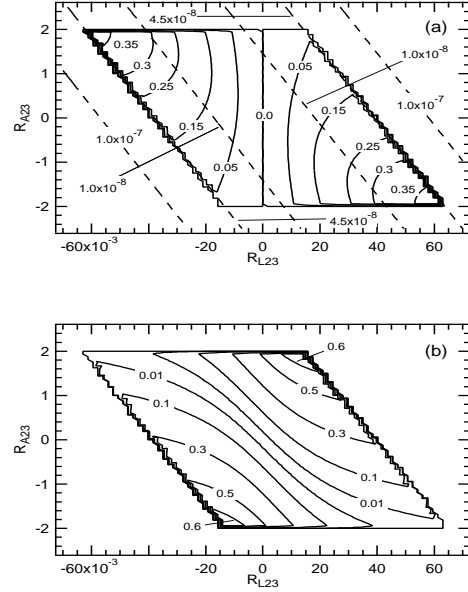


Fig. 3. Contours of the LFV decay branching ratios (a) $B(\tilde{\nu}_2 \rightarrow \tau^- \tilde{\chi}_1^+)$ and (b) $B(\tilde{\nu}_2 \rightarrow \tilde{\ell}_1^- H^+)$ in the $R_{L23} - R_{A23}$ plane for our $\tilde{\mu} - \tilde{\tau}$ mixing scenario. The region with no solid contours is excluded by the conditions (i) to (v) given in the text. The dashed lines in (a) show contours of $B(\tau^- \rightarrow \mu^- \gamma)$.

play an important role in determination of the LFV parameters $M_{L,23}^2$ and A_{23} .

In Fig.4 we show a scatter plot of the LFV decay branching ratios $B(\tilde{\nu}_2 \rightarrow \tilde{\ell}_1^- H^+)$ versus $B(\tau^- \rightarrow \mu^- \gamma)$ for our $\tilde{\mu} - \tilde{\tau}$ mixing scenario with the parameters $M_2, \mu, R_{L23}, R_{E23}, R_{A23}$ and R_{A32} varied in the ranges $0 < M_2 < 1000$ GeV, $|\mu| < 1000$ GeV, $|R_{L23}| < 0.1$, $|R_{E23}| < 0.2$, $|R_{A23}| < 2.5$ and $|R_{A32}| < 2.5$, satisfying the conditions (i) to (v) given above. All parameters other than $M_2, \mu, M_{L,23}^2, M_{E,23}^2, A_{23}$ and A_{32} are fixed as in the reference scenario specified above. As can be seen in Fig.4, the LFV branching ratio $B(\tilde{\nu}_2 \rightarrow \tilde{\ell}_1^- H^+)$ could go up to 30% even if the present bound on $B(\tau^- \rightarrow \mu^- \gamma)$ improves by one order of magnitude. For the other LFV decay branching ratios of $\tilde{\nu}_{1,2}$ versus $B(\tau^- \rightarrow \mu^- \gamma)$ we have obtained scatter plots sim-

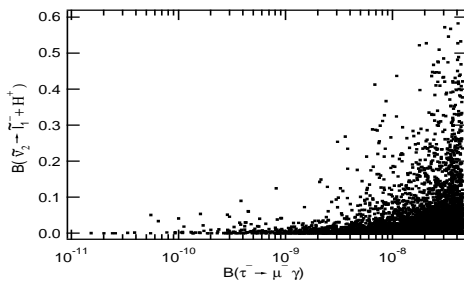


Fig. 4. Scatter plot of the LFV decay branching ratios $B(\tilde{\nu}_2 \rightarrow \tilde{\ell}_1^- H^+)$ versus $B(\tau^- \rightarrow \mu^- \gamma)$ for our $\tilde{\mu} - \tilde{\tau}$ mixing scenario.

ilar to that for $B(\tilde{\nu}_2 \rightarrow \tilde{\ell}_1^- H^+)$ versus $B(\tau^- \rightarrow \mu^- \gamma)$, with the upper limits of the $\tilde{\nu}_{1,2}$ decay branching ratios $B(\tilde{\nu}_1 \rightarrow \mu^- \tilde{\chi}_1^+) \lesssim 0.12$, $B(\tilde{\nu}_1 \rightarrow \tilde{\ell}_2^- H^+) \lesssim 0.40$, $B(\tilde{\nu}_1 \rightarrow \tilde{\ell}_2^- W^+) \lesssim 0.05$, $B(\tilde{\nu}_2 \rightarrow \tau^- \tilde{\chi}_1^+) \lesssim 0.35$, and $B(\tilde{\nu}_2 \rightarrow \tilde{\ell}_1^- W^+) \lesssim 0.22$. Note that $B(\tilde{\nu}_1 \rightarrow \tilde{\ell}_2^- H^+)$ can be very large due to sizable $M_{E,23}^2$, A_{32} and large A_{33} .

We have also studied sneutrino decay branching ratios in the case of $\tilde{e} - \tilde{\tau}$ mixing, where we have obtained similar results to those in the case of $\tilde{\mu} - \tilde{\tau}$ mixing. This is due to the fact that $Y_{E,11} \sim Y_{E,22} (\sim 0)$, that the experimental limits on $B(\tau^- \rightarrow e^- \gamma)$ and $B(\tau^- \rightarrow \mu^- \gamma)$ are comparable, and that the theoretical limits of the condition (i) on the LFV parameters A_{13} and A_{31} are also similar to those on A_{23} and A_{32} .

4.2 LFV contributions to collider signatures

It is to be noted that in $\tilde{e} - \tilde{\tau}$ mixing scenario the t -channel chargino exchanges contribute significantly to the cross sections $\sigma(e^+e^- \rightarrow \tilde{\nu}_i \tilde{\nu}_j) \equiv \sigma_{ij}$ for $i, j = 1, 3$, enhancing the cross sections (including the LFV production cross section σ_{13}) strongly, where $\tilde{\nu}_1 \sim \tilde{\nu}_\tau$ and $\tilde{\nu}_3 \sim \tilde{\nu}_e$ [2]. We have studied the LFV contributions to signatures of sneutrino production and decay at the ILC [2]. We have shown that the LFV processes (including the LFV $\tilde{\nu}_i$ productions and the LFV bosonic $\tilde{\nu}_i$ decays also) can contribute significantly to signal event rates. For example, in the $\tilde{e} - \tilde{\tau}$ mixing scenario described in [2], assuming ILC with $\sqrt{s} = 1$ TeV and a longitudinal polarization of -90% and 60% for the electron and positron beam, respectively, the dominant LFV contributions (stemming from $e^+e^- \rightarrow \tilde{\nu}_i \tilde{\nu}_j \rightarrow e^\pm \tau^\mp \tilde{\chi}_1^+ \tilde{\chi}_1^-$) to the rate of the signal event $e^\pm \tau^\mp + 4\text{jets} + \cancel{E}$ is calculated to be $\sigma^{LFV} = 6.6\text{fb}$, where \cancel{E} is the missing energy. Lepton flavour conserving (LFC) processes in $\tilde{\nu}$ production and decay can also contribute to the rate of the signal event above. The dominant LFC contributions to the signal rate is calculated to be $\sigma^{LFC} = 0.033\text{fb}$ which is two orders of magnitude smaller than σ^{LFV} . This strongly suggests that one should take into account the possibility of the significant contributions of both the LFV fermionic and bosonic decays in the sneutrino search

and should also include the LFV parameters in the determination of the basic SUSY parameters at colliders. It is clear that detailed Monte Carlo studies taking into account background and detector simulations are necessary. However, this is beyond the scope of the present article.

5 Summary

We have performed a systematic study of sneutrino production and decays including both fermionic and bosonic decays in the general MSSM with slepton generation mixings. We have shown that LFV sneutrino production cross sections and LFV sneutrino decay branching ratios can be quite large due to slepton generation mixing in a significant part of the MSSM parameter space despite the very strong experimental limits on LFV processes. This could have an important impact on the search for sneutrinos and the MSSM parameter determination at future colliders, such as LHC, ILC, CLIC and muon collider.

Acknowledgements

I sincerely thank the other authors of [2]: A. Bartl, K. Hohenwarter-Sodek, T. Kernreiter, W. Majerotto and W. Porod.

References

1. A. Bartl, H. Eberl, K. Hidaka, S. Kraml, T. Kon, W. Majerotto, W. Porod, and Y. Yamada, Phys. Lett. B **460**, (1999) 157; A. Bartl, K. Hidaka, T. Kernreiter, W. Porod, Phys. Lett. B **538**, (2002) 137 [arXiv:hep-ph/0204071]; A. Bartl, K. Hidaka, T. Kernreiter and W. Porod, Phys. Rev. D **66**, (2002) 115009 [arXiv:hep-ph/0207186].
2. A. Bartl, K. Hidaka, K. Hohenwarter-Sodek, T. Kernreiter, W. Majerotto and W. Porod, arXiv:0709.1157 [hep-ph].
3. For example, see references in [2].
4. J.A. Casas and S. Dimopoulos, Phys. Lett. B **387**, (1996) 107 [arXiv:hep-ph/9606237].
5. M. L. Brooks *et al.* [MEGA Collaboration], Phys. Rev. Lett. **83**, (1999) 1521 [arXiv:hep-ex/9905013].
6. K. Abe *et al.* [Belle Collaboration], Proceedings of The 33rd International Conference on High Energy Physics (ICHEP 06), Moscow, Russia, 26 Jul - 2 Aug 2006 [arXiv:hep-ex/0609049].
7. B. Aubert *et al.* [BABAR Collaboration], Phys. Rev. Lett. **96**, (2006) 041801 [arXiv:hep-ex/0508012].
8. U. Bellgardt *et al.* [SINDRUM Collaboration], Nucl. Phys. B **299**, (1988) 1.
9. K. Abe *et al.* [Belle Collaboration], arXiv:0708.3272.
10. W. M. Yao *et al.* [Particle Data Group], J. Phys. G **33**, (2006).
11. F. Jegerlehner, arXiv:hep-ph/0703125.
12. K. Ikado *et al.* (Belle Collaboration), Phys. Rev. Lett. **97**, (2006) 251802 [arXiv:hep-ex/0604018v3].
13. J. Hisano, T. Moroi, K. Tobe and M. Yamaguchi, Phys. Rev. D **53**, (1996) 2442.